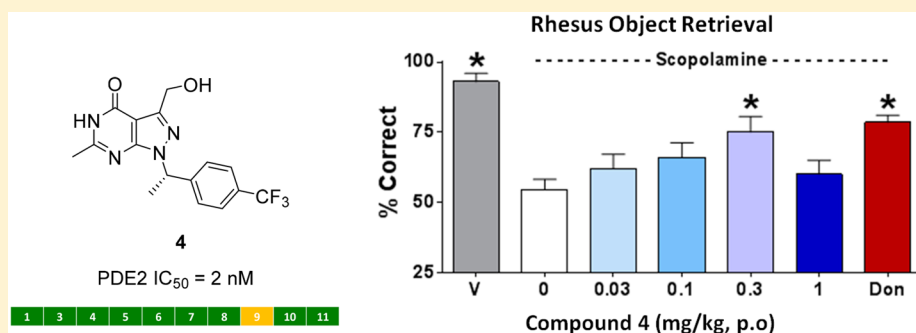


Structure-Guided Design and Procognitive Assessment of a Potent and Selective Phosphodiesterase 2A Inhibitor

Shawn J. Stachel,*¹ Richard Berger, Ashley B. Nomland, Anthony T. Ginnetti, Daniel V. Paone, Deping Wang, Vanita Puri, Henry Lange, Jason Drott, Jun Lu, Jacob Marcus, Michael P. Dwyer, Sokreine Suon, Jason M. Uslaner, and Sean M. Smith

Merck & Co. Inc., P.O. Box 4, West Point, Pennsylvania 19486, United States

Supporting Information



ABSTRACT: Herein we describe the development of a series of pyrazolopyrimidinone phosphodiesterase 2A (PDE2) inhibitors using structure-guided lead identification and design. The series was derived from informed chemotype replacement based on previously identified internal leads. The initially designed compound 3, while potent on PDE2, displayed unsatisfactory selectivity against the other PDE2 isoforms. Compound 3 was subsequently optimized for improved PDE2 activity and isoform selectivity. Insights into the origins of PDE2 selectivity are described and verified using cocrystallography. An optimized lead, 4, demonstrated improved performance in both a rodent and a nonhuman primate cognition model.

KEYWORDS: Structure-guided design, PDE2, schizophrenia, cognition

Schizophrenia is a chronic debilitating disorder estimated to affect approximately one percent of the world population. Disease onset begins in late adolescence and early adulthood. Patients suffer from a cluster of symptoms, generally subdivided into positive symptoms, negative symptoms, and cognitive dysfunction. Positive symptoms include hallucinations, delusions, and agitated behavior. Negative symptoms consist of anhedonia and lack of motivation. Cognitive dysfunction includes impaired episodic and working memory, executive functioning, and attention. Some reports estimate the indirect costs associated with cognitive deficits are substantially greater than the direct costs for treating psychotic symptoms as they are the primary contributor to homelessness, joblessness and suicide.¹ Unfortunately, currently available antipsychotics only target positive symptoms with either slight or no efficacy on the other domains. There are also significant adverse effects (AE's) associated with these treatments leading to a high rate of discontinuation due to dissatisfaction with efficacy and lack of tolerability. As such there is a need to develop novel antipsychotics to treat cognitive disturbances associated with schizophrenia with greater efficacy and reduced AEs.

A potential therapeutic target we chose to investigate for cognitive dysfunction was a group of enzymes known as phosphodiesterase's (PDE's).^{2,3} This protein class is respon-

sible for the hydrolysis of cyclic adenosine monophosphate (cAMP) and cyclic guanosine monophosphate (cGMP). cAMP and cGMP are important secondary messengers involved in regulating intracellular signaling cascades. Inhibition of phosphodiesterase activity results in increased intracellular cAMP/cGMP levels thereby amplifying signal propagation involved in these pathways. With the recent discovery of PDE12⁴ there are currently 12 known families of PDEs (PDE1–12) which are grouped by their cyclic nucleotide substrate preferences for cAMP, cGMP, or both cAMP and cGMP. Importantly, the homology in the catalytic domain between the families is modest, ranging from 20% to 45%, suggesting the possibility to design isoform selective inhibitors. PDE2, a dual cAMP/cGMP hydrolase, is expressed heavily in brain regions thought to be involved in cognition, including the hippocampus and prefrontal and perirhinal cortex. Importantly, schizophrenics show deficits on tasks that rely on these brain regions. In addition, pharmacological inhibition of PDE2 has been shown to improve performance in

Received: May 9, 2018

Accepted: July 26, 2018

Published: July 26, 2018

rodent behavioral assays of learning and memory and several compounds have progressed into clinical trials.^{5–7}

In an attempt to cast a wide and diverse net for lead identification we employed a variety of lead finding approaches including high-throughput screening (HTS), fragment-based screening, and structure-guided lead design. We have recently reported on inhibitor series that were identified using the two former screening methods, fragment-based screening and HTS, i.e. compounds **1** and **2** in Figure 1.^{7,8} Herein we describe the third method used for lead identification, that of structure-guided lead design.

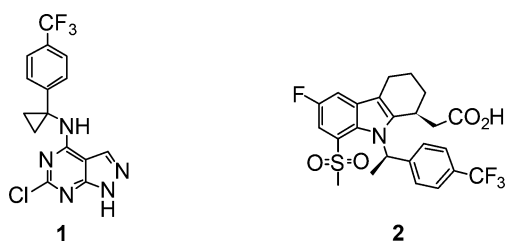


Figure 1. Previously reported PDE2 inhibitors.

With the binding insights gained from selectivity and cocrystallographic data of inhibitors in the PDE2 active site from previous publications, we set out to design alternative heterocyclic cores incorporating the selectivity elements garnered from previous efforts.^{8,9} Compound **3** depicts one such attempt where the pyrazolopyrimidinone from the previously reported elaborated fragment lead **1** was replaced with a pyrazolopyrimidinone in an attempt to make alternative hydrogen-bonding interactions within the PDE2 active site. The pyrazolopyrimidinone scaffold also allows for facile incorporation of the para-CF₃ benzyl group, which has been shown to occupy a hydrophobic binding-induced pocket between Ile866 and Leu770. This binding pocket is unique to PDE2 and its occupation contributes to inhibitor isoform selectivity.^{8–10} Compound **3** was found to have potent PDE2 activity, IC₅₀ = 23 nM, and maintained the favorable ligand efficiency present in compound **1** (compound **1** HPLC LogD = 2.7, LE = 0.45, LLE = 4.02; compound **3** HPLC LogD = 2.7, LE = 0.45, LLE = 4.93). However, the selectivity profile versus the other PDE isoforms was less than desired with selectivity against PDE9 the lowest at only 4-fold. The colored bar in Figure 2 below the structures depicts a selectivity heatmap to visualize isoform selectivity for PDE's 1–11 where red represents a selectivity ratio of 0–100-fold, orange 101–500-fold, and green >500-fold. Using in silico methods to dock compound **3** into the PDE2 active site suggested that the lack of selectivity likely stemmed from nonproductive interactions

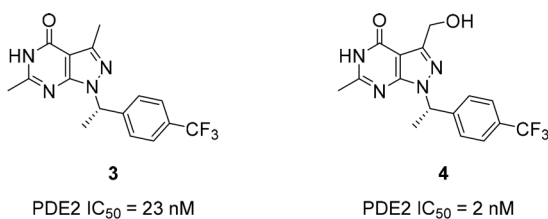


Figure 2. Structure-guided lead generation and selectivity profiles.

of the methyl group in the 3-position of the pyrazolopyrimidinone with Gln812 as depicted in Figure 4.

In this regard, the glutamine residue at position 859 is conserved throughout the PDE family, whereas the glutamine at position 812 is unique to PDE2 compared to the other PDE isoforms. Figure 3 is a listing of the resident amino acids at

PDEX	1	2	3	4	5	6	7	8	9	10	11
AA	Pro	Gln	Pro	Pro	Ile	Val	Pro	Pro	Glu	Val	Ile

Figure 3. PDE isoform amino acid residue 812 identity.

position 812 between the differing PDE homologues. Most of the PDE homologues contain either a proline residue at position 812, as seen in PDE 1, 3, 4, 7, and 8, or another lipophilic amino acid such as valine or isoleucine as is seen in PDE 6, 10, 5, and 11. In our previously published selective pyrazolopyrimidinone inhibitor series, compound **1**, glutamine 812 was observed to be engaged in a water-mediated hydrogen-bond with the N-2 nitrogen of the pyrazolopyrimidinone leading to increased PDE isoform selectivity for this compound shown in green in Figure 4. In contrast, compound

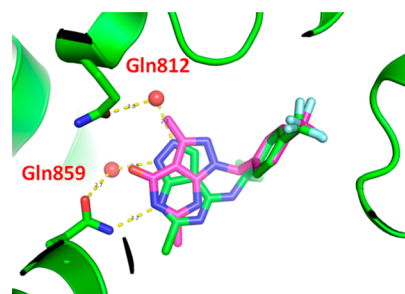


Figure 4. Docking overlay of compound **3** (magenta) with compound **1** (green).

3, shown in magenta, contains a methyl substituent at the three position. This hydrophobic methyl group effectively displaces the water molecule leading to nonproductive interactions with the polar glutamine side-chain group in PDE2 as compared to favorable hydrophobic interaction the 3-methyl substituent can make with the PDE isoforms with lipophilic substituents at residue 812, thereby negatively effecting selectivity.

We hypothesized that the addition of a polar group in the 3-position of compound **3** capable of forming a hydrogen bonding interaction with Gln812, and potentially negative binding interaction with lipophilic residues at this position in other PDE isoforms, would lead to an enhanced selectivity profile. In further support of this hypothesis, in a WaterMap¹¹ analysis of compound **1**, the water molecule interacting with Gln812 is not thermodynamically stable and has a high ΔG of 10.5 kcal/mol relative to bulk water, suggestive of the potential to replace the water molecule with a direct hydrogen bond while maintaining or improving PDE2 potency.

To test this hypothesis, compound **4**, containing a hydroxymethyl group at the 3-position of the pyrazolopyrimidinone was synthesized in an attempt to engage Gln812 in a constructive direct hydrogen-bonding interaction. Gratifyingly, in addition to this modification affording a 10-fold improvement in PDE2 potency over compound **3**, IC₅₀ = 2 nM, it also significantly enhanced the selectivity versus other PDE2 isoforms.¹² Now selectivity ratios of greater than 500-fold

were observed over all PDE2 isoforms except PDE9, and even this selectivity ratio was increased from 4-fold for compound 3 to 315-fold for compound 4. A direct hydrogen-bonding interaction of the 3-hydroxyl group in 4 with Gln812 was confirmed by cocrystallization with PDE2. Figure 5 displays

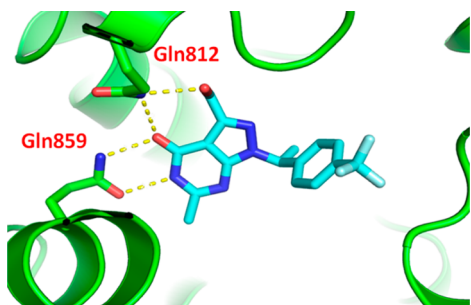


Figure 5. Co-crystal structure of compound 4 in the PDE2 active site.

the interaction of compound 4 in the PDE2 active site where, in addition to the 3-hydroxyl interacting with Gln812, the pyrimidinone oxygen is also now more proximal to Gln812, 3.2 Å, most likely providing further selectivity enhancement.

The addition of the hydroxyl group also served to lower the LogD of compound 4 (HPLC LogD = 2.2) compared to compound 3 (HPLC LogD = 2.7) which, when coupled with the increase in potency, resulted in a further improvement in ligand binding efficiency (LE = 0.48, LLE = 6.48). Compound 4 also displayed good microsomal stability (HLM $CL_{int,s} < 6.2$ mL/min/kg) and pharmacokinetic properties in rats supportive of in vivo pharmacodynamic studies (Cl = 5.6 mL/min/kg; $t_{1/2}$ = 2.9 h; V_{dss} = 1.4 L/kg; %F = 84%; rat PPB = 85%). In addition, 4 also exhibited a favorable ancillary profile with no ion channel or cyp activity (IC_{50} 's > 50 μ M), no significant activities (i.e., IC_{50} or EC_{50} > 10 μ M) in a broad spectrum Cereps Panlabs panel, and minimal ppg efflux, which suggested acceptable brain penetration (Pgp efflux ratio = 1.0 human, 3.0 rat; P_{app} = 37×10^{-6} cm/s). Compound 4 was subsequently administered to rats to gauge its ability to elevate cyclic nucleotide levels in brain tissue as a demonstrable pharmacodynamic marker. Thirty minutes after oral administration of either 3, 10, or 30 mg/kg, brain tissue was harvested and frozen for measurement of cGMP. All three dose levels resulted in significant elevation of cortical cGMP levels compared to controls, as shown in Figure 6. It should be noted that the doses required to observe cyclic nucleotide changes in brain tissue are often much higher than those necessary to see behavioral effects due to the limited ability to detect changes in cGMP over background.

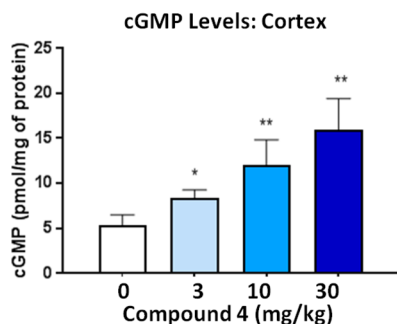


Figure 6. Effects of compound 4 on cGMP levels in rat brain.

Having demonstrated a robust pharmacodynamic response through increased cyclic GMP levels in the brain, compound 4 was evaluated in a rodent behavioral model, the novel object recognition (NOR) test, for its ability to improve recognition memory. The NOR task is performed by exposing vehicle- or scopolamine-treated rats to two identical objects. Then the animals are exposed 1 h later to one of the objects they had previously been exposed to and one novel object. Untreated rats, without an induced deficit, will spend more time exploring a novel object than a familiar one, indicating recognition of the familiar object. However, scopolamine impairs normal recognition memory such that rats explore both the familiar and novel object equally. As noted above, behavioral effects often require lower doses than those required to observe significant pharmacological modulation of end points and as such the starting doses for this study were reduced compared with those in Figure 6. As seen in Figure 7, compound 4

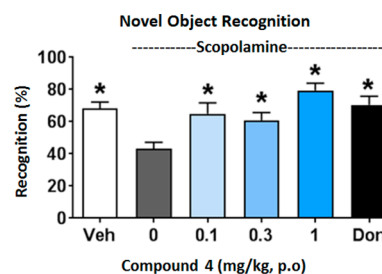


Figure 7. Compound 4 in scopolamine-impaired Novel Object Recognition in adult rats.

significantly reversed the effect of scopolamine and improved episodic memory in novel object recognition at all dose levels tested, 0.1, 0.3, and 1 mg/kg, where the effect was comparable to that of donepezil, the positive control used in the assay.

Having demonstrated robust efficacy in a rodent cognition model, compound 4 was subsequently assessed for utility in a nonhuman primate model of cognition and was found to display pharmacokinetic properties supportive of in vivo rhesus pharmacodynamic studies (Cl = 2 mL/min/kg; $t_{1/2}$ = 5.2 h; V_{dss} = 0.88 L/kg; %F = 100%; rhesus PPB = 90%). As such, compound 4 was evaluated in the scopolamine-impaired Rhesus Object Retrieval (OR) assay (Figure 8), a prefrontal cortex-dependent task of executive function.^{13,14} In this assay the subject is tasked with retrieving a food object placed deep inside a clear box with a single open side that is not in the direct view of the subject. Attempts are scored as correct or incorrect depending on whether the subject was able to retrieve the food without touching a closed side of the box. As

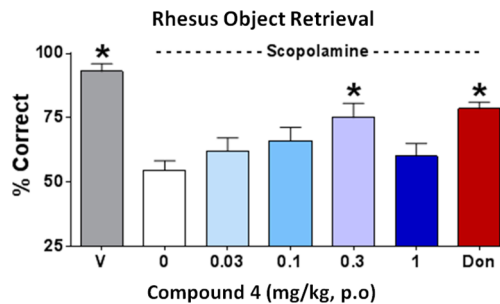


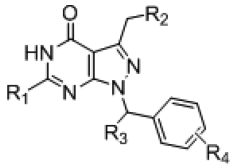
Figure 8. Compound 4 in scopolamine-impaired Rhesus Object Retrieval in adult monkeys.

with the NOR rodent assay, scopolamine administration results in decreased performance on the task. Compound **4** was able to reverse the scopolamine-induced deficit and subjects exhibited a higher percentage of correct scores compared to untreated (scopolamine alone) subjects. The assay displayed a dose dependent increase in reversal of the scopolamine impairment achieving a comparable effect to positive control donepezil at the 0.3 mg/kg dose. Reduced efficacy was observed at the highest dose of 1 mg/kg, an effect often observed with preclinical cognitive function and memory assays.¹⁵

In summary, compound **4** exhibited excellent PDE2 potency, high selectivity versus other PDE isoforms, a clean ancillary profile, and low Pgp efflux.¹⁶ In addition, **4** exhibited excellent pharmacokinetic properties in multiple species and improved cognitive performance in both the rat Novel Object Recognition and rhesus Object Recognition assays and as such was advanced as a potential preclinical candidate for further studies.

While we were able to rapidly identify compound **4** as a potent and selective compound of interest using structure-guided design, we subsequently investigated additional SAR for this series (Table 1). As seen in compound **5**, PDE activity in

Table 1. Additional Series SAR



Cmpd	R ₁	R ₂	R ₃	R ₄	PDE2 IC ₅₀ (nM)
5	CH ₃	OH	(<i>R</i>)-Me	<i>p</i> -CF ₃	216
6	CH ₃	OH	(<i>S</i>)- <i>t</i> Bu	<i>p</i> -CF ₃	9
7	CH ₃	OH	(<i>S</i>)-Me	<i>m</i> -F, <i>p</i> -CF ₃	1.3
8	3,4-OMe Bz	OH	(<i>S</i>)-Me	<i>p</i> -CF ₃	0.89
9	OH	OH	(<i>S</i>)-Me	<i>p</i> -CF ₃	14
10	OH	F	(<i>S</i>)-Me	<i>p</i> -CF ₃	2
11	OH	CF ₃	(<i>S</i>)-Me	<i>p</i> -CF ₃	0.96

the series resides primarily in the *S*-enantiomers with the *R*-enantiomer substantially less active, IC₅₀ = 216 nM. Selectivity against other PDE's was not determined for **5** since the assay ceiling was 30 μM but **5** displayed little activity against the other PDE isoforms. Additional SAR at R₃ revealed that small branched alkyls were well tolerated and analogs displayed similar potency and selectivity to compound **4**, and in some cases such as compound **6** where R₃ = *t*-butyl, selectivity versus PDE9 was even slightly enhanced. SAR for R₄ was consistent with previously published SAR where hydrophobic para-substituents were tolerated.^{8,9} One notable example was compound **7** where an additional meta-fluorine substituent on the CF₃-aryl ring led to a slight increase in potency and a further enhancement in selectivity over PDE9 to 950-fold. R1

could also be substituted with a variety of alkyl groups while maintaining PDE2 potency with varying levels of isoform selectivity. Notably, introduction of a 3,4-dimethoxy benzyl substituent at R₁ (**8**), which is present in the BAY60-7550 PDE inhibitor,¹⁰ resulted in only a slight increase in PDE2 activity, IC₅₀ = 0.89 nM, and a decrease in selectivity against PDE5 and **8** compared to compound **4**. However, the addition of the dimethoxy benzyl group also resulted in a large increase in Pgp susceptibility with Pgp efflux ratios of 11 for human and 35 for rat. Hence a simple methyl substituent was the preferred group from both a ligand efficiency and Pgp susceptibility perspective. Interestingly, replacement of the 6-methyl R₁ substituent on compound **4** with a hydroxyl group to give compound **9** affected only a modest loss in PDE2 activity, IC₅₀ = 14 nM, but results in a further increase in its selectivity profile with selectivity ratios now greater than 1000-fold against all other isoforms tested. Notably PDE9 selectivity was increased to 1193-fold for compound **9** vs 314-fold for compound **4**. Examination of the cocrystallographic complex of compound **9** in the PDE2 active site revealed that the 6-hydroxyl substituent participates in an additional water-mediated hydrogen-bond to Tyr827 (Figure 9). As this

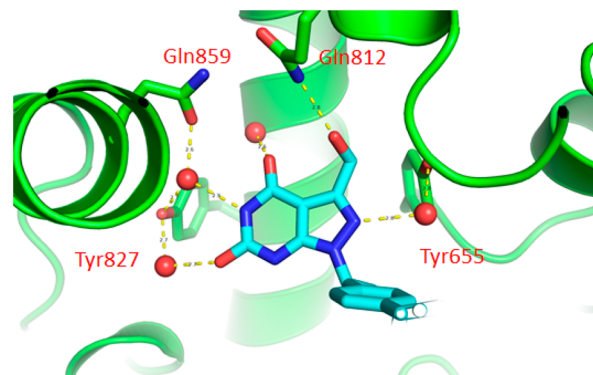


Figure 9. Co-crystal structure of compound **9** bound in the PDE2 active site.

residue is a leucine in PDE9, the repulsive hydrogen-bond donor interaction with the hydrophilic leucine residue likely contributes to the enhanced selectivity now seen against this isoform. The change from methyl to hydroxyl also lowered the LogD of **9** to 1.1, resulting in an additional increase in LLE to 6.61 and did not deleteriously affect Pgp susceptibility.¹⁷

R₂ was then investigated with the inclusion of the R₁ hydroxyl as a potency and selectivity standard for the series. Here the R₂ hydroxyl in compound **9**, shown to exhibit hydrogen-bonding interactions with Gln812, was replaced with a fluorine atom to give compound **10** while maintaining a high selectivity profile. However, selectivity was slightly degraded toward PDE9 where the ratio dropped from greater than 1000-fold for compound **9** to 445-fold, PDE9 IC₅₀ = 899 nM, for compound **10**. Even more interesting, compound **10** resulted in 7-fold improved PDE2 potency, IC₅₀ = 2 nM, versus the analogous hydroxyl compound **9**.

The selectivity results observed with compound **10** suggested that the fluorine substituent may be participating in a hydrogen-bond with Gln812.¹⁸ As such, the trifluoromethyl derivative was synthesized with the thought of decreasing the entropic penalty needed for orientation of the 3-fluoro substituent toward Gln812. The replacement of the R₂ fluorine in compound **10** with a trifluoromethyl group, to

give compound **11** resulted in yet a further increase in PDE2 potency, $IC_{50} = 0.96$ nM. More importantly, not only was the attractive selectivity profile restored compared to compound **9** but it was even further enhanced with compound **11** displaying selectivity of greater than 12000-fold against all of the PDE2 isoforms! In addition, the CF_3 group only increased the LogD to 1.8 from compound **9**, LogD = 1.1, which is still lower than that of compound **4**, LogD = 2.7, and when combined with its potency compound **11** exhibits good ligand efficiency metrics with LE = 0.43 and a LLE = 7.03. At first we hypothesized that the selectivity and potency may be a result of a tetral bonding interaction where the trifluoromethyl group acts as a σ -hole donor and forms a noncovalent bond with an appropriate Lewis base, i.e. the oxygen of Gln812. Tetral bonding interactions with trifluoromethyl groups have been observed in other protein–ligand complexes in the protein data bank (PDB), albeit infrequently, with one particular example of a tetral interaction with an asparagine as the binding partner.¹⁹ However, upon closer inspection of the cocrystal structure, the orientation of the Gln812 carbonyl is nonlinear with the α -hole of the CF_3 . A more plausible explanation for the enhanced potency and selectivity may be that the fluorines of the CF_3 substituent are involved in direct hydrogen-bonding interactions with Gln812, of which two fluorines can be observed in hydrogen-bonding distance to Gln812 in the cocrystal structure (Figure 10). In addition, the third fluorine atom is

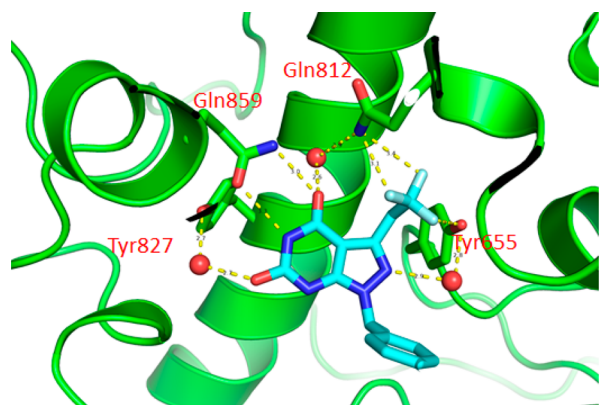
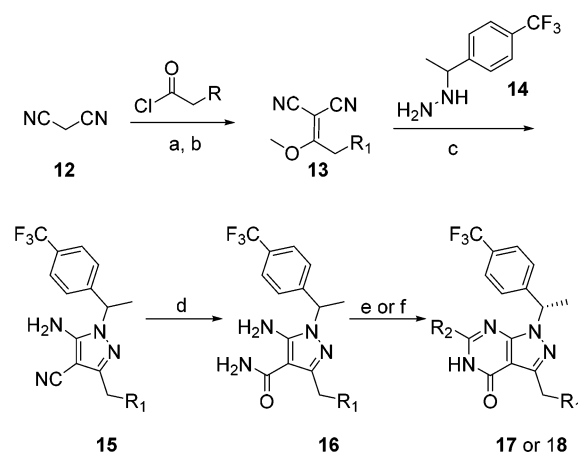


Figure 10. Co-crystal structure of compound **11** bound in PDE2 active site.

observed to be in close distance (3.1 Å) to the hydroxyl group of Tyr655, suggesting another possible hydrogen–fluorine hydrogen-bond. This interaction may also result in increased selectivity against PDE9, where this residue is a phenylalanine instead of a tyrosine residue. Unfortunately, in addition to the increases in potency and selectivity, compound **11** also exhibited increased Pgp susceptibility, and Pgp efflux ratio = 4.8 human, 19 rat, limiting its utility. However, this interaction may be useful as a design element for other ligand systems that have interactions with asparagine or glutamine residues.

Compounds were synthesized as depicted in Scheme 1. The synthesis starts with condensation of malononitrile and the appropriately substituted acid chloride (R is hydrogen for compound **3**, *O*-benzyl for compound **4** and **9**, fluorine for compound **10**, and trifluoromethyl for compound **11**) using sodium hydride to give an enolic intermediate that is subsequently converted to the methyl enol ether **13** via acid catalyzed exchange with trimethyl orthoformate. Intermediate

Scheme 1. Convergent Synthetic Route to 6-Methyl and 6-Hydroxy Pyrazolopyrimidinone Compounds



13 is then condensed under basic protic conditions with hydrazine **14** to afford amino pyrazole **15**. The nitrile group is then hydrolyzed to the corresponding primary amide using basic peroxide conditions to provide **16**.²⁰ Intermediate **16** is then either condensed with acetyl chloride to provide the corresponding 6-methyl pyrazolopyrimidinones (**17**) or reacted with triphosgene to provide the 6-hydroxy pyrazolopyrimidinones (**18**).

In summary, starting with a pyrazolopyrimidine chemical series identified through fragment-based screening, we employed a core modification strategy using structure-guided design to establish a novel pyrazolopyrimidinone series with sufficient potency and selectivity to serve as a starting point for series optimization. Selectivity against other PDE isoforms was increased by leveraging cocrystallographic data to optimize critical hydrogen-bonding interactions within the active site. Compound **4** emerged as a potent and highly selective lead with a clean ancillary profile and good brain penetration properties. In addition, compound **4** exhibited excellent pharmacokinetic properties in multiple species and in vivo pharmacodynamic studies where it demonstrated efficacy and improved cognitive performance in both the rat novel object recognition and rhesus object retrieval assays.

■ ASSOCIATED CONTENT

Supporting Information

The Supporting Information is available free of charge on the ACS Publications website at DOI: 10.1021/acsmchemlett.8b00214.

Experimental procedures and compound characterization data (PDF)

■ AUTHOR INFORMATION

Corresponding Author

*Phone: 215-652-2273. E-mail: shawn_stachel@merck.com.

ORCID

Shawn J. Stachel: 0000-0002-5392-582X

Notes

The authors declare no competing financial interest. Structure coordinates have been deposited in the Protein Data Bank (PDB): codes 6CYB, 6CYC, 6CYD.

■ ABBREVIATIONS

Cyp,cytochromes P450; Don,donepezil; HLM,human liver microsomes; LE,ligand efficiency; LLE,lipophilic ligand efficiency; P-gp,p-glycoprotein; PPB,plasma protein binding

■ REFERENCES

- (1) Harvey, P. D.; Strassnig, M. Predicting the Severity of Everyday Functional Disability in People with Schizophrenia: Cognition Deficits, Functional Capacity, Symptoms, and Health Status. *World of Psychiatry* **2012**, *11*, 73–79.
- (2) Gomez, L.; Breitenbucher, J. G. PDE2 Inhibition: Potential for the Treatment of Cognitive Disorders. *Bioorg. Med. Chem. Lett.* **2013**, *23*, 6522–6527.
- (3) Wu, Y.; Li, Z.; Huang, Y.-Y.; Wu, D.; Luo, H.-B. Novel Phosphodiesterase Inhibitors for Cognitive Improvement in Alzheimer's Disease. *J. Med. Chem.* **2018**, *61*, 5467–5483.
- (4) Poulsen, J. B.; Andersen, K. R.; Kjaer, K. H.; Vestergaard, A. L.; Justesen, J.; Martensen, P. M. Characterization of Human Phosphodiesterase 12 and Identification of a Novel 2'-5' Oligoadenylate Nuclease - The Ectonucleotide Pyrophosphatase/Phosphodiesterase 1. *Biochimie* **2012**, *94*, 1098–1107.
- (5) Boess, F. G.; Hendrix, M.; van derStaay, F.-J.; Erb, C.; Schreiber, R.; van Staveren, W.; de Vente, J.; Prickaerts, J.; Blokland, A.; Koenig, G. Inhibition of Phosphodiesterase 2 Increases Neuronal cGMP Synaptic Plasticity and Memory Performance. *Neuropharmacology* **2004**, *47*, 1081–1092.
- (6) Helal, C. J.; Arnold, E.; Boyden, T.; Chang, C.; Chappie, T. A.; Fisher, E.; Hajos, M.; Harms, J. F.; Hoffman, W. E.; Humphrey, J. M.; Pandit, J.; Kang, Z.; Kleiman, R. J.; Kormos, B. L.; Lee, C.-W.; Lu, J.; Maklad, N.; McDowell, L.; McGinnis, D.; O'Connor, R. E.; O'Donnell, C. J.; Ogden, A.; Piotrowski, M.; Schmidt, C. J.; Seymour, P. A.; Ueno, H.; Vansell, N.; Verhoest, P. R.; Yang, E. X. Identification of a Potent, Highly Selective, and Brain Penetrant Phosphodiesterase 2A Inhibitor Clinical Candidate. *J. Med. Chem.* **2018**, *61*, 1001–1018.
- (7) Mikami, S.; Nakamura, S.; Ashizawa, T.; Nomura, I.; Kawasaki, M.; Sasaki, S.; Oki, H.; Hoffman, I. D.; Zou, H.; Uchiyama, N.; Nakashima, K.; Kamiguchi, N.; Imada, H.; Suzuki, N.; Iwashita, H.; Taniguchi, T. Discovery of Clinical Candidate N-((1S)-1-(3-Fluoro-4-(trifluoromethoxy)phenyl)-2-methoxyethyl)-7-methoxy-2-oxo-2,3-dihydropyrido[2,3-b]pyrazine-4(1H)-carboxamide (TAK-915): A Highly Potent Selective, and Brain-Penetrating Phosphodiesterase 2A Inhibitor for the Treatment of Cognitive Disorders. *J. Med. Chem.* **2017**, *60*, 7677–7702.
- (8) Stachel, S. J.; Egbertson, M. S.; Wai, J.; Machacek, M.; Toolan, D. M.; Swestock, J.; Eddins, D. M.; Puri, V.; McGaughey, G.; Su, H.-P.; Perlow, D.; Wang, D.; Ma, L.; Parthasarathy, G.; Reid, J. C.; Abeywickrema, P. D.; Smith, S. M.; Uslander, J. M. Indole Acids as a Novel PDE2 Inhibitor Chemotype that Demonstrate Pro-Cognitive Activity in Multiple Species. *Bioorg. Med. Chem. Lett.* **2018**, *28*, 1122–1126.
- (9) Forster, A. B.; Abeywickrema, P.; Bunda, J.; Cox, C. D.; Cabalu, T. D.; Egbertson, M.; Fay, J.; Getty, K.; Hall, D.; Kornienko, M.; Lu, J.; Parthasarathy, G.; Reid, J.; Sharma, S.; Shipe, W. D.; Smith, S. M.; Soisson, S.; Stachel, S. J.; Su, H.-P.; Wang, D.; Berger, R. The Identification of a Novel Lead Class for Phosphodiesterase 2 Inhibition by Fragment-Based Drug Design. *Bioorg. Med. Chem. Lett.* **2017**, *27*, 5167–5171.
- (10) Zhu, J.; Yang, Q.; Dai, D.; Huang, Q. J. X-ray Crystal Structure of Phosphodiesterase 2 in Complex with a Highly Selective, Nanomolar Inhibitor Reveals a Binding-Induced Pocket Important for Selectivity. *J. Am. Chem. Soc.* **2013**, *135*, 11708–11711.
- (11) Cappel, D.; Sherman, W.; Beuming, T. Calculating Water Thermodynamics in the Binding Site of Proteins – Applications of WaterMap to Drug Discovery. *Curr. Top. Med. Chem.* **2017**, *17*, 2586–2598.
- (12) During the preparation of this manuscript another report using late-stage functionalization of a triazinone based PDE2 inhibitor was reported. Interestingly, in this case the addition of the 3-hydroxyl to the methyl group only resulted in a slight increase in PDE2 activity, 2-fold vs the 10-fold increase we observed going from compound 3 to 4: Stepan, A. F.; Tran, T. P.; Helal, C. J.; Brown, M. S.; Chang, C.; O'Connor, R. E.; De Vivo, M.; Doran, S. D.; Fisher, E. L.; Jenkinson, S.; Karanian, D.; Kormos, B. L.; Sharma, R.; Walker, G. S.; Wright, A. S.; Yang, E. X.; Brodney, M. A.; Wager, T. T.; Verhoest, P. R.; Obach, R. S. Later-Stage Microsomal Oxidation Reduces Drug-Drug Interaction and Identified Phosphodiesterase 2A Inhibitor PF-06815189. *ACS Med. Chem. Lett.* **2018**, *9*, 68–72.
- (13) Eddins, D.; Hamill, T. G.; Puri, V.; Cannon, C. E.; Vivian, J. A.; Thompson, F.; Uslander, J. M. The Relationship between Glycine Transporter 1 Occupancy and the Effects of the Glycine Transporter 1 Inhibitor RG1678 or ORG25935 on Object Retrieval Performance in Scopolamine Impaired Rhesus Monkey. *Psychopharmacology* **2014**, *231*, 511–519.
- (14) Uslander, J. M.; Eddins, D.; Puri, V.; Sutcliffe, J.; Chew, C. S.; Pearson, M.; Vivian, J. A.; Chang, R. K.; Ray, W. J.; Kuduk, S. D.; Wittmann, M. The Muscarinic M1 Receptor Positive Allosteric Modulator PQCA Improves Cognitive Measures in Rat, Cynomolgus Macaque, and Rhesus Macaque. *Psychopharmacology* **2013**, *225*, 21–30.
- (15) Baldi, E.; Bucherelli, C. The Inverted “U-Shaped” Dose-Effect Relationships in Learning and Memory: Modulation of Arousal and Consolidation. *Nonlinearity Biol., Toxicol., Med.* **2005**, *3*, 9–21.
- (16) Brain binding was not measure for compound 4 but CSF/unbound plasma drug levels were measured to be ~1:4 in rat across various dose levels. This ratio of 1:4 CSF/plasma was also observed in Pgp KO rats, suggesting Pgp was not the limiting factor for equitable CSF/unbound plasma levels susceptibility of 4 to other transport mechanisms was not explored.
- (17) Pgp efflux ratio = 0.32 human, 0.38 rat; $P_{app} = 41 \times 10^{-6}$ cm/s. While the pgp efflux ratio was low in the assay, it was determined that 9 was not a substrate for MDR1 or MDR1A Pgp efflux.
- (18) Zhou, P.; Zou, J.; Tian, F.; Shang, Z. Fluorine Bonding – How Does it Work in Protein-Ligand Interactions. *J. Chem. Inf. Model.* **2009**, *49*, 2344–2355.
- (19) McIsaac, J. E.; Ball, R. E.; Behrman, E. J. The Mechanism of the Base-Catalyzed Conversion of Nitriles to Amides by Hydrogen Peroxide. *J. Org. Chem.* **1971**, *36*, 3048–3050.
- (20) Garcia-Llinas, X.; Bauza, A.; Seth, S. K.; Frontera, A. Importance of R-CF3-O Tetrel Bonding Interactions in Biological Systems. *J. Phys. Chem. A* **2017**, *121*, 5371–5376.